Coalescence phenomena in 1D silver nanostructures

2009 J. Phys.: Condens. Matter 21 295301

(http://iopscience.iop.org/0953-8984/21/29/295301)

J. Phys.: Condens. Matter **21** (2009) 295301 (9pp) doi:10.1088/0953-8984/21/29/295301

Coalescence phenomena in 1D silver nanostructures

C Gutiérrez-Wing[1], M Pérez-Alvarez[1,2], G Mondragón-Galicia[1], J Arenas-Alatorre[3], M T Gutiérrez-Wing[4], M C Henk[5], I I Negulescu[6,7] and K A Rusch[4]

[1] Instituto Nacional de Investigaciones Nucleares, Carretera México-Toluca S/N La Marquesa, Ocoyoacac, Estado de México, CP 52750, Mexico
[2] Centro de Investigación en Materiales Avanzados, Miguel de Cervantes No. 120, Complejo Industrial Chihuahua, Chihuahaua, Chih. 31109, Mexico
[3] Instituto de Física, UNAM, Apartado Postal 20-364, 01000 México DF, Mexico
[4] Civil and Environmental Engineering, Louisiana State University, Baton Rouge, LA 70803, USA
[5] Socolofsky Microscopy Center, Department of Biological Sciences, 202 Life Sciences Building, Louisiana State University, Baton Rouge, LA 70803, USA
[6] Department of Chemistry, 232 Choppin Hall, Louisiana State University, Baton Rouge, LA 70803, USA
[7] School of Human Ecology, 125 Human Ecology Building, Louisiana State University, Baton Rouge, LA 70803, USA

E-mail: claudia.gutierrez@inin.gob.mx

Received 29 December 2008, in final form 15 May 2009
Published 3 July 2009
Online at stacks.iop.org/JPhysCM/21/295301

Abstract
Different coalescence processes on 1D silver nanostructures synthesized by a PVP assisted reaction in ethylene glycol at 160 °C were studied experimentally and theoretically. Analysis by TEM and HRTEM shows different defects found on the body of these materials, suggesting that they were induced by previous coalescence processes in the synthesis stage. TEM observations showed that irradiation with the electron beam eliminates the boundaries formed near the edges of the structures, suggesting that this process can be carried out by the application of other means of energy (i.e. thermal). These results were also confirmed by theoretical calculations by Monte Carlo simulations using a Sutton–Chen potential. A theoretical study by molecular dynamics simulation of the different coalescence processes on 1D silver nanostructures is presented, showing a surface energy driven sequence followed to form the final coalesced structure. Calculations were made at 1000–1300 K, which is near the melting temperature of silver (1234 K). Based on these results, it is proposed that 1D nanostructures can grow through a secondary mechanism based on coalescence, without losing their dimensionality.

1. Introduction

A number of applications have been found for one-dimensional (1D) nanostructures due to their unique magnetic, optic, electronic and catalytic properties. These findings have opened the possibility to construct sensors [1–3] and connectors in nanoscale devices [4], attracting the attention of many scientists and technologists of different fields. However, their performance, related mainly to transport properties, is dependent on features such as structure, defects and other surface characteristics, that are determined during their synthesis process. In order to understand and optimize their preparation and applications, extensive research regarding the growth and formation of 1D silver nanostructures has been reported, mainly through the synthesis in ethylene glycol by a PVP (polyvinylpyrrolidone) assisted reaction [5–7]. Even when the exact mechanism of formation of these materials has not been completely understood, most investigations evidence the presence of fcc 1D Ag nanostructures with pentagonal symmetry [8]. Among the proposed growth mechanisms, it has been reported that these 1D nanostructures begin with the formation of a decahedral nanoparticle,

followed by the aggregation of subsequent decahedral nanoparticles on vertices of the former decahedron on the [111] direction [6], continuing this process until a 1D nanostructure is formed. In this kinetically controlled growth, it has been mentioned that PVP acts as a growth director of the 1D structures, capping preferential planes of the silver crystal as it grows, these being the {100}, leaving the {111} faces free to continue growing [7, 8], which are the ones exposed on the tip of the decahedral 1D structures.

Based on experimental observations, it has been noticed that, regardless of the initial steps to form the 1D nanostructures, other processes such as coalescence can contribute to their growth, modifying their structural characteristics and leaving typical defects on the body of these structures. Some of the defects can be identified as 'knee-like defects'; others are viewed as boundaries between the two coalesced structures, or atomic rearrangement zones as discussed on this paper. Coalescence between nanoparticles has been reported before [10]; however, this behavior is not always similar to the process followed when a 1D nanostructure is taking part in these phenomena. Here we report the study of different coalescence processes either between 1D nanostructures or by a nanoparticle and a 1D nanostructure, by transmission electron microscopy (TEM), high resolution transmission electron microscopy (HRTEM), and molecular dynamics simulation, suggesting that some of the remaining defects are originated by this coalescence phenomenon, which can be eliminated by means of energy input into the system. Coalescence between 1D and 0D nanostructures was followed in situ in the TEM, where characteristic defects were observed at the end of the process. These results allowed us to identify defects on the 1D nanostructures right after their synthesis, indicating that their formation occurred as a consequence of coalescence in the synthesis stage. TEM defect observation on the 1D nanostructures immediately after their preparation suggested that coalescence between 1D structures can happen, as an intermediate stage in the formation of the final product. Obtained results lead us to propose that different types of coalescence can contribute to the growth of the final 1D silver nanostructures by a secondary mechanism.

2. Experimental details

2.1. Synthesis of 1D Ag nanostructures

1×10^{-4} mmol of H_2PtCl_6 in 1 ml H_2O were mixed with 20 ml of ethylene glycol at 160 °C. Under vigorous stirring, 0.01 mmol of polyvinylpyrrolidone (PVP) were added simultaneously with 1.0 mmol of $AgNO_3$. The product was precipitated in acetone and the final product was suspended in ethanol.

For the characterization by transmission electron microscopy (TEM), a drop of the sample was deposited over a carbon coated TEM copper grid and the analysis was performed in JEOL-2010 HT, JEOL-2010 FEG and JEOL-100CX transmission electron microscopes.

2.2. Theoretical procedure

Theoretical analysis of the studied nanomaterials was performed by molecular dynamic simulation [11, 12]. This procedure was based on three fundamental steps:

(a) Generation of the geometrical models. Starting from a geometrical basis, the atomic positions of the nanostructures are predicted guided by crystallographic indices and multilayered ensembles [13]. Simulated decahedral rods are conformed by 2055 atoms.
(b) The geometrical models generated are taken to a local state of minimum energy by means of an optimization algorithm.
(c) The molecular dynamics simulation is performed by the Monte Carlo method starting from two models of particles of minimum energy [14], following the process behavior [15] and energy changes in the structures, from 1000 to 1300 K.

The generation of models of minimum potential energy and the molecular dynamic simulation studies were guided by the evaluation of the potential energy of the system described by the Sutton–Chen [16] many-body interaction potential.

Monte Carlo simulations were based on the acceptance or rejection of different events calculated per iteration, where each event is related to the change in the atomic position in the simulated model as a consequence of temperature. In order to accept an event, the simulated model with the new atomic position has to reach a certain energy threshold determined by the Boltzmann statistics [17], otherwise the event is rejected. After a number of iterations have been calculated, a vibration of the atoms is observed. These atomic vibrations calculated by Monte Carlo method occur at a picosecond timescale; however, these calculations take long computational times. Usually, models studied by this method are composed of a few hundred atoms [18, 19]. A larger number of atoms will lead to longer calculation times, since timescale increases exponentially as a function of the number of atoms [20, 21]. In order to reach a change in the average atomic positions, many vibrations have to occur.

The studied temperatures were determined based on the melting temperature of silver, 1234 K, where mobility of the atoms can be achieved. At 1000 K the atoms start having significant mobility, which leads to coalescence; however, the atomic rearrangement process can be stalled. In order to be free from stalling and avoid metastable states [22, 23], temperature has to be increased. Studies were carried out up to 1300 K. Higher temperature will lead to the destruction of the model. At temperatures lower than 1000 K not enough mobility of the atoms is achieved, so the coalescence cannot take place in reasonable computing times.

These studies considered the analysis of the simulated nanostructures suspended in vacuum, with the only purpose of showing the atomic arrangement modifications that take place as the coalescence process develops, when the planes of each nanostructure approach. The sizes of the modeled structures allow observation of the critical section of the coalescing structures, where the rearrangement takes place. Longer nanostructures will only be affected near the contacting planes,

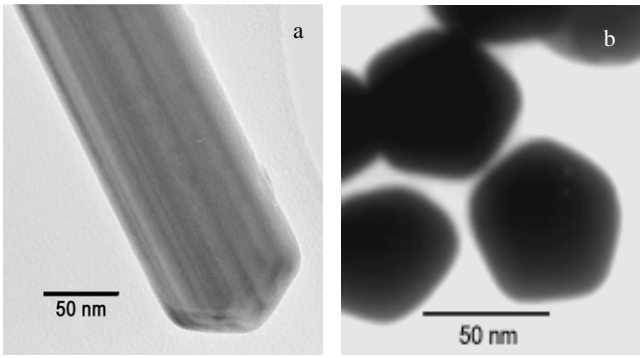

Figure 1. TEM image of a 1D nanostructure with pentagonal symmetry. (a) Longitudinal view, (b) transversal view.

as observed experimentally, since the farther atoms are not modified by the coalescence process at the studied conditions.

3. Results

1D silver wires were obtained with the method described above. As reported previously [5–7], 1D decahedral structures such as the one presented in figure 1 were commonly found. The pentagonal symmetry of these structures is observed in the transversal view image of figure 1(b). Simultaneously, other less common structures were also obtained (e.g. single twin).

Regardless of the type of geometry of the fibers synthesized by this method, analysis by TEM showed that, once the 1D silver nanostructures were formed, common defects such as the ones presented below were found on the body of the material, suggesting their formation as a consequence of coalescence processes between different nanostructures during the synthesis stage.

This coalescence might be influenced by the tip shapes of the 1D nanostructures, since the energy of the exposed facets differs from an edge, a vertex or a more stable round-structure, leading to either linear or angular 1D nanostructures [10]. TEM observations allowed the determination of some structural differences on the tip of the 1D nanostructures, identifying round-shaped ends as in figure 2(a), less rounded–faceted (2(b)) and angular–pointed tips (2(c)). All three types can have different degrees of truncation.

Analysis of these structures and species with other morphologies found during the synthesis process led to the identification of different coalescence types as explained below. Since decahedral 1D structures were the most commonly found, analysis was made based on these 1D nanostructures with pentagonal symmetry.

Case I: coalescence between a 1D nanostructure and a nanoparticle

This case is explained by following the diffusion process *in situ* under TEM observations, where mobility of the nanoparticles was detected over the carbon substrate of the TEM grid. Two different coalescence situations were identified.

(a) These phenomena were found between a nanoparticle and a 1D nanostructure where the coalescing nanoparticle has a significantly smaller cross-section than the 1D nanostructure (figure 3). It can be seen that when the nanoparticle is small its atoms are incorporated into the 1D structure until almost every atom of the nanoparticle has rearranged over the (111) surface of the fiber and no noticeable boundary defect between the two initial structures can be observed. In this case, the heat released as a consequence of the coalescence process is enough to induce the rearrangement of the small particle's atoms.

This type of coalescence was followed *in situ* under TEM observations and is similar to that presented between two nanoparticles, one with a cross-section considerably smaller than the other, previously reported by Yacaman *et al* [9]. Theoretical analysis of this behavior, based on the calculation

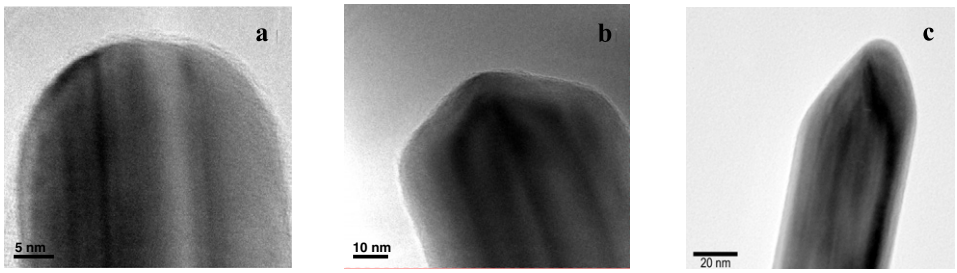

Figure 2. Different end shapes found in 1D nanostructures.

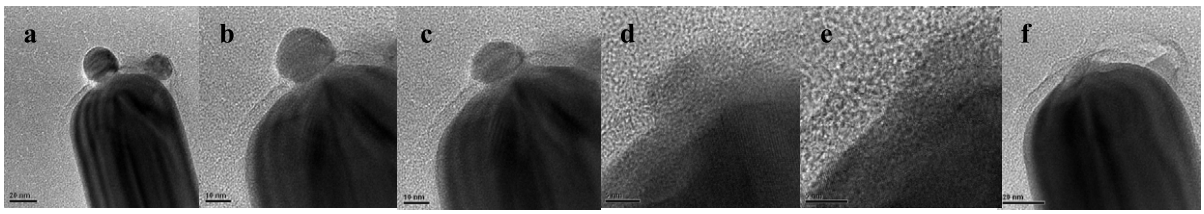

Figure 3. Coalescence sequence between a small nanoparticle and a large cross-section 1D nanostructure. Observe in (f) that there is no noticeable boundary between the two coalesced nanostructures.

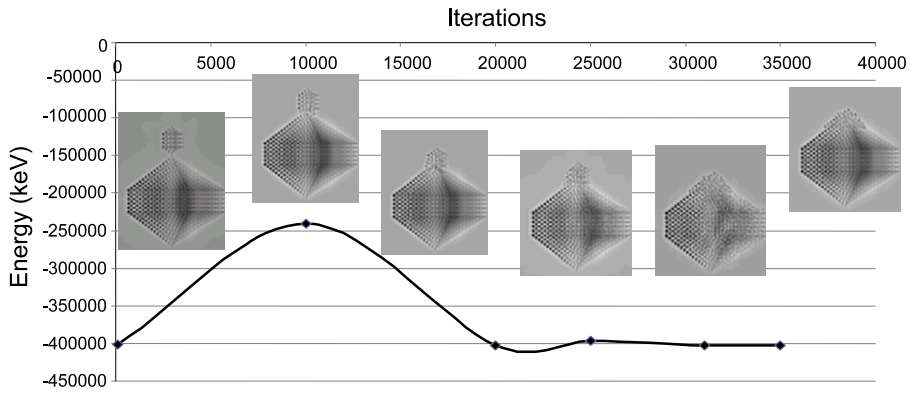

Figure 4. Energy calculation of the coalescence process of a small decahedral nanoparticle and a 1D decahedral nanostructure of larger cross-section.

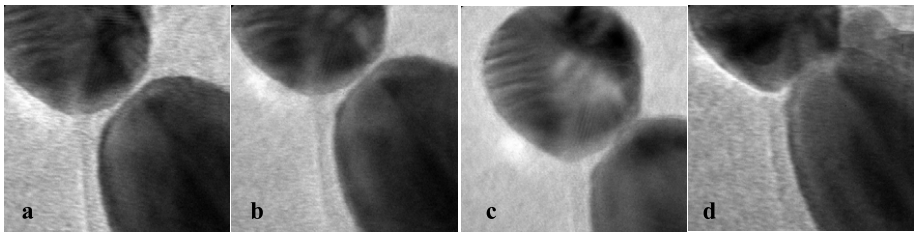

Figure 5. Coalescence sequence between a 0D and a 1D nanostructure with similar cross-sections.

of the energy of the system at each stage of the coalescence process, is presented in figure 4. It is observed from these results that the small nanoparticle starts reorganizing its atoms over the (111) surfaces of the larger decahedral nanoparticle; however, a minimum energy state is reached when the organization stops and no more energy changes are registered. Even when there is not a noticeable boundary between the two coalesced nanostructures, still there is evidence of the process. This describes clearly the same experimental observations of figure 3.

(b) A second coalescence process between a 0D and a 1D nanostructure was based on an already formed 1D structure of decahedral geometry and a nanoparticle where both structures have the same cross-section (figure 5). In this case the process begins with a slight flattening of the structures on the contacting planes (figure 5(b)), followed by a neck-like formation, as in the coalescence of two nanoparticles (figure 5(c)) [9, 10]. The nanoparticle suffers a small deformation once it has made contact with the 1D nanostructure as observed in figure 5(c): notice how the side near the 1D nanostructure tends to increase its length and gets narrower on that side until the contacting planes match in shape, leaving a planar defect as a boundary between the original species. This process was followed under TEM observation and it was seen that once the structures have coalesced a planar defect remains on the new structure formed. In this case the energy required to rearrange the atoms in either structure turns out to be higher than that available under the conditions studied, since the number of atoms is too high to allow this restructuration, and also the released energy during the coalescence is not enough to favor a complete rearrangement of the atomic planes. Figure 6 presents a coalesced structure produced by this type of coalescence.

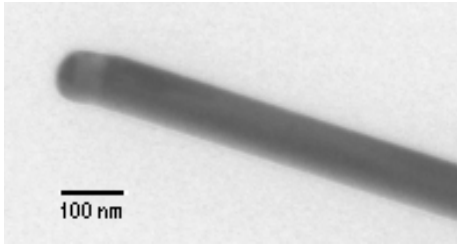

Figure 6. Note the planar defect remaining after coalescence of 0D and 1D structures with a similar cross-section.

Theoretical calculations lead to similar results, and allow observation that higher reorganization of the atoms between both structures would not be energetically favorable, leaving a clear defect between the two coalesced nanostructures, since, as shown after stage (e) of figure 7, the energy of the system increases, suggesting that in order to reach this stage it is necessary to apply some energy.

The study of coalescence followed *in situ* by TEM allows us to observe the final defect found after the process has evolved. Such defects were also found on the samples right after the preparation process, indicating that it is possible to have these coalescence events during the synthesis stage, as evidenced in the image of figure 6.

Case II: coalescence between 1D structures

Analysis of the defects found on the 1D nanostructures right after the preparation procedure suggest that they were originated as a consequence of coalescence processes between two parent 1D nanostructures. Some of these defects were similar to those in case I.

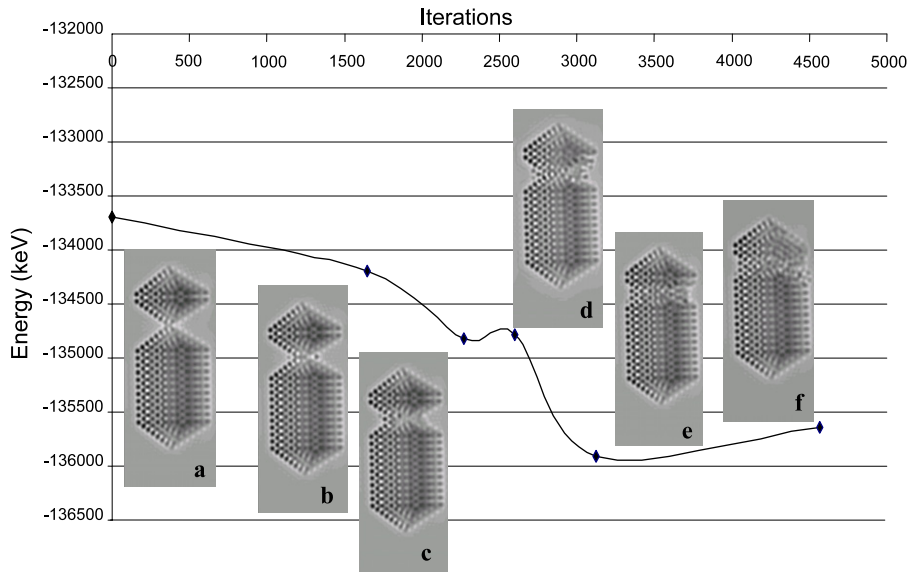

Figure 7. Coalescence sequence between 0D and 1D nanostructures with similar cross-sections, obtained by molecular dynamics simulation. Observe the energy decrease as the coalescence process is developed until it reaches a minimum (e) and then increases again.

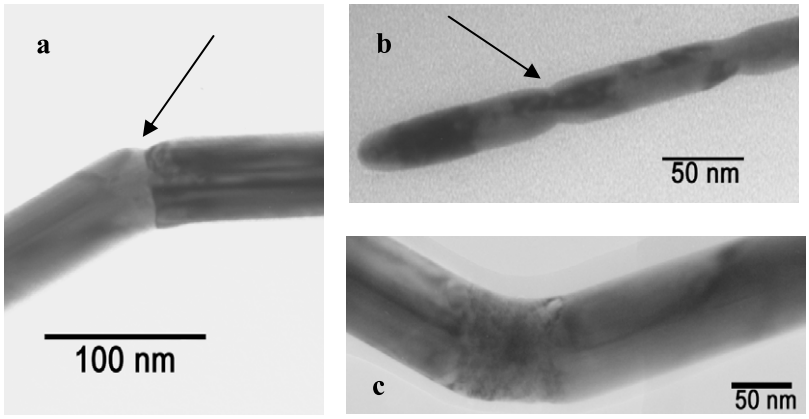

Figure 8. Coalescence of two 1D nanostructures. (a) The arrow indicates a planar defect defining an angle on the structure. (b) Longitudinal cross-section. Note the clear groove defect pointed out by the arrow. (c) Reordering of the structure after coalescence, defining a greater angle on the structure.

Mobility of 1D nanostructures was not detected under TEM observations, indicating that the coalescence phenomena observed between 1D structures was originated from the synthesis stage. Coalescence between 1D nanostructures can be interrupted at different stages of interfacial reorganization, yielding different types of defects, depending on the degree of rearrangement of the atoms at the interface once the process has stopped. This reorganization can be influenced by the structural (morphological) features of the coalescing tips, hence the reason why some angles are observed in coalesced nanostructures.

Types of defects

(a) The first type corresponds to well identified planar defects located transversally on the 1D nanostructures, which can be described as groove boundaries between two 1D nanostructures [24]. This case presents similarities with the coalescence between a 1D nanostructure and a nanoparticle with the same cross-section described above (figure 5). This phenomenon is shown in figures 8(a) and (b), where the coalescence between two 1D nanostructures creates a longer fiber where the boundary between them is clearly noticed and indicated by the arrow. The contacting planes during coalescence in figure 8(a) were not perpendicular to the growth direction, hence the reason why an angle is formed in the boundary. The longitudinal cross-section image in figure 8(b) shows how the defect is located across the fiber as pointed out in the image, where a curvature on the edges of the groove evidences the two original 1D nanostructures that have coalesced in the growth direction of both structures.

(b) The second type. Another defect observed in the structures is presented in figure 8(c), where the coalescence process creates an angle in the structure. Reordering of atoms after coalescence is defined by a greater area. This defect could

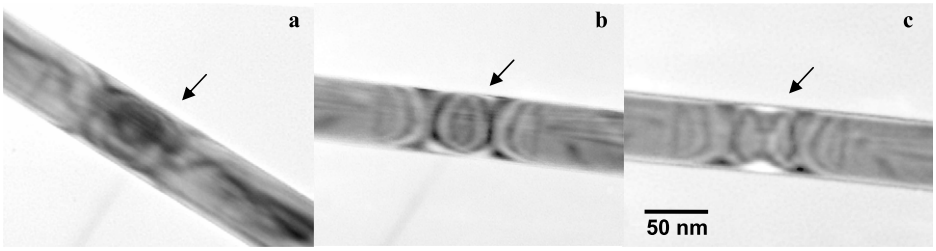

Figure 9. Defocus series on a knee-like defect found on 1D nanostructures, leading to strain on the structures as pointed out by the arrows. Notice the neck formation in the middle of the structure.

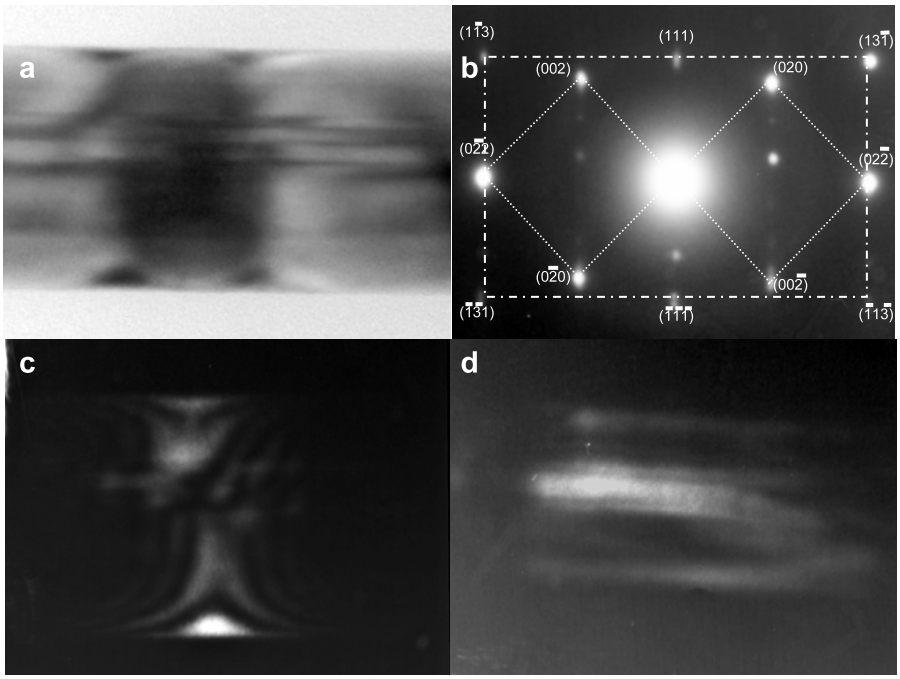

Figure 10. (a) TEM image of a 1D nanostructure showing a knee-like defect. (b) Electron diffraction pattern of the defective area in (a). (c), (d) Dark field imaging constructed with reflection of planes (111) and (0$\bar{2}$2), respectively.

have been originated by the coalescence of two (111) planes not perpendicular to the growth direction of the nanostructure, leading to an angular coalesced structure as demonstrated below with theoretical calculations in figure 12.

(c) The third type. Some of these defects show a 'knee-like' contrast as presented in figures 9(a)–(c). Concentric fringes near each defect are observed at low magnification, suggesting a reorganization of the crystal after coalescence between two 1D nanostructures. Defocus series from 9(a) to 9(c) allow observation of a neck formed in the middle of the defect, and the less contrasted areas around the neck indicate that the thickness of the structure is different as indicated in figure 9(c); however, a constant contrast is always observed in the middle of the structure. The electron diffraction pattern taken from the knee-like defective area shows the superposition of two electron diffraction patterns with the directions [100] and [2$\bar{1}\bar{1}$] respectively of the cubic system from silver with a lattice parameter of $a = 0.4086$ nm, in agreement with the findings reported by Xia and Yang [5]. The electron dark field imaging with reflections (0$\bar{2}$2) and (111) in the electron diffraction pattern with direction [2$\bar{1}\bar{1}$] is shown in figures 10(c) and (d). From this analysis a difference in thickness was observed between the center of the knee-like region and the wedges on the sides of the 1D nanostructure on the defective area. It is shown that the twinning plane parallel to [111] in the middle of the structure is already formed (figures 10(a) and (d)), suggesting a higher degree of ordering of the atoms along the longitudinal central section of the structure, even when the sides still have wedges of unfilled sections. Also, it is observed that planes (0$\bar{2}$2) corresponding to the transversal section are still under rearrangement (figure 10(c)), causing the knee-like type of defects.

Coalescence between two decahedral 1D nanostructures was studied by molecular dynamics simulation. Notice that the last two stages of the simulated process are very similar to what was observed in figure 8. First a transition zone where reorganization of atoms takes place, as indicated in stage (e) of figure 11, then an identified planar defect, similar to the last HRTEM simulated image on the last stage of this figure.

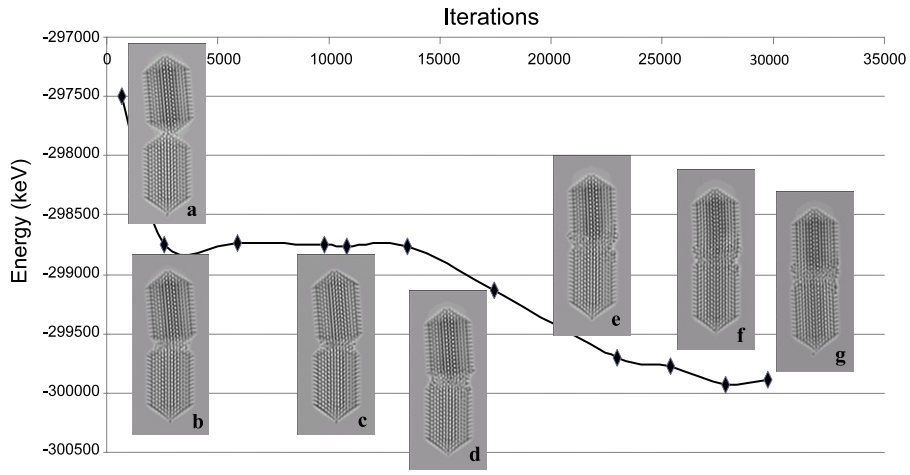

Figure 11. Coalescence between decahedral 1D structures obtained by molecular dynamics simulation. The approach is made between the tips of the nanostructures.

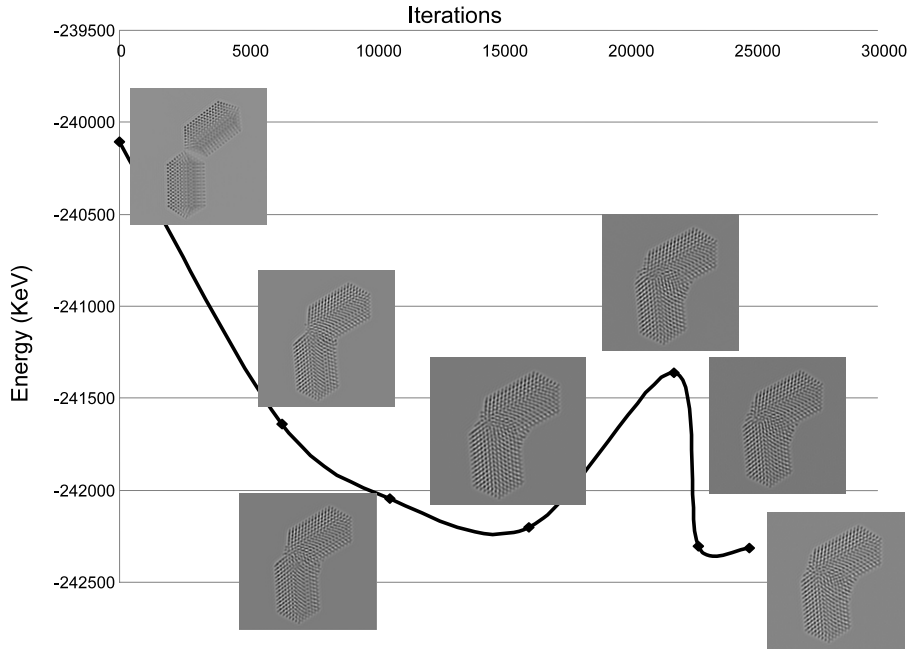

Figure 12. Coalescence between decahedral 1D structures obtained by molecular dynamics simulation. The approach is made between the (111) planes of the nanostructures.

It is also possible to have angular 1D nanostructures, formed as a consequence of coalescence when the two contacting planes are not perpendicular to the growth direction, as presented in case II (b). Figure 12 shows the simulated process of coalescence between two 1D nanostructures where the contact approach is flat between two (111) planes. Notice how the process develops leaving a structure similar to that observed in figure 8(c).

The simulated sequences were studied on 1D nanostructures of the same size, with the only purpose of showing the atomic arrangement as coalescence proceeds. The process was stopped when these modifications allow us to understand the phenomena without compromising the integrity of the 1D character. Since these theoretical models are very small in comparison with the real nanostructures, further computer processing will finally lead to structures of spherical tendency, energetically more stable.

4. Discussion

Based on TEM observations, it was found that the characteristic defects identified on the 1D nanostructures might have been originated from a surface energy driven coalescence process between structures of different dimensionality present in the reaction system, where the type of defect depends on the structures taking part in the process. The reorganization of atoms depends on the size of the coalescing structures. It was found that when one of the coalescing structures has a

dimension of a few nanometers [9, 10] this interaction allows the alignment of the nanoparticle atoms over the contacting planes of the 1D nanostructure, incorporating its atoms on the lattice of these latter. However, coalescence was more likely observed between the tips of the decahedral nanofibers, over the {111} planes of the structures [25], than between the transversal facets. This can be explained in terms of differences in surface energy of these two sides and the interaction of PVP over (100) and (111) planes. In this regard, it has been reported that these (111) facets of the silver 1D nanostructures remain with a high chemical potential and reactivity [26, 27] due to a weaker interaction of the O (and/or N) from PVP, in comparison with the longitudinal side planes (100). This results in a favored aggregation process on the tips of the structures, where the potential energy is modified [28], and where there is more likely to be an interaction in order to reduce the energy of the system. Calculations were made over 226 atom surfaces to determine the surface energy on both sides of a simulated decahedral 1D silver nanostructure of 6033 atoms, obtaining a potential energy of (−1202 keV) and (−1160 keV) over the (100) and (111) planes respectively. The presence of more edges and a vertex on the tip contributes to a higher reactivity in comparison with the atoms in the longitudinal planes (atoms with fewer neighbors are atoms less strongly bounded).

The different coalescence phenomenon presented here can be viewed as a secondary growth mechanism of the 1D metallic nanostructures. The fact that some of the 1D structures are not straight and the angle shown is formed where a defect is located can be explained based on the fact that not all the tips are flat and the coalescence depends on the first contacting facets of both nanostructures, which also affect the angle between them. Simulation of the process presented the coalescence approach from two limits, tips (figure 11) and planes (figure 12).

When the energy released from the coalescence process is not enough to rearrange all the atoms in the contacting planes of both species taking part in the process, the final structure cannot reach a minimum energy state by aligning the atomic planes of both structures under the studied synthesis conditions. However, as theoretical analysis showed, in order to reach a less defective structure, the energy of the system tends to increase (figures 7 and 11), suggesting that to be able to eliminate the defects some energy must be applied. This was corroborated in the TEM, after the defective structures were irradiated with the electron beam and immediately only the defects near the tips run short distances along the structure until they disappeared on the tip. This explains the fact that some coalescence typical defects remain on the newly formed 1D nanostructures, which were observed as dark fringes, pointed out in the image of figure 9. These findings suggested that some other means of energy could be applied to reduce the number of coalescence defects, which might cause a poor performance, mainly in transport properties.

5. Conclusions

Coalescence evidence between nanostructures with different tip shapes and dimensionalities has been presented here. These two features have influenced the type of defects present on the final structure, leading to the growth of 1D nanostructures by a secondary mechanism, regardless of the structures and shapes of the initial materials taking part in the coalescence process. The coalescence process between 0D and 1D followed *in situ* in the TEM allowed us to identify characteristic defects left by this phenomenon in the synthesized 1D nanostructures. Also, based on the analysis of defects found on the body of the synthesized 1D nanostructures and theoretical calculations, coalescence between 1D nanostructures was identified. Theoretical studies confirm this surface energy driven mechanism, and the fact that in order to eliminate the defects on the structures some form of energy must be applied.

Acknowledgments

This work was supported by ININ through project CA-712 and by CONACYT through project J-49603. The authors thank MSc Isidoro Martinez Mera and L Rendón for their technical assistance in the TEM, and LAMC Maria Eufemia Fernandez García for valuable discussions.

References

[1] Shanmukh S, Jones L, Driskell J, Zhao Y, Dluhy R and Tripp R A 2006 *Nano Lett.* **6** 2630
[2] Li X, Gao H, Murphy C J and Caswell K K 2003 *Nano Lett.* **3** 1495–8
[3] Graff A, Wagner D, Ditlbacher H and Kreibig U 2005 *Eur. Phys. J.* D **34** 263–9
[4] Maddanimath T, Kumar A, D'Arcy-Gall J, Ganesan P G, Vijayamohanan K and Ramanath G 2005 *Chem. Commun.* 1435–7
[5] Xia Y and Yang P 2003 *Adv. Mater.* **15** 351
[6] Reyes-Gasga J, Elechiguerra J L, Liu C, Camacho-Bragado A, Montejano-Carrizales J M and Jose-Yacaman M 2006 *J. Cryst. Growth* **286** 162–72
[7] Andrew P and Ilie A 2007 *J. Phys.: Conf. Ser.* **61** 36–40
[8] Gao Y, Song L, Jiang P, Liu L F, Yan X Q, Zhou Z P, Liu D F, Wang J X, Yuan H J, Zhang Z X, Zhao X W, Dou X Y, Zhou W Y, Wang G, Xie S S, Chen H Y and Li J Q 2005 *J. Cryst. Growth* **276** 606–12
[9] José-Yacamán M, Gutierrez-Wing C, Miki M, Yang D Q, Piyakis K N and Sacher E 2005 *J. Phys. Chem.* B **109** 9703–11
[10] Palasantzas G, Vystavel T, Koch S A and De Hosson J Th M 2006 *J. Appl. Phys.* **99** 24307
[11] Rodrigues V and Ugarte D 2002 *Nanotechnology* **13** 404–8
[12] Iijima S and Ichihashi T 1986 *Phys. Rev. Lett.* **56** 616–9
[13] Zhou G *et al* 2006 *J. Cryst. Growth* **289** 255–9
[14] Ni C, Hassan P A and Kaler E W 2005 *Langmuir* **21** 3334–7
[15] Wang Y, Teitel S and Dellago C 2007 *J. Comput. Theor. Nanosci.* **4** 282–90
[16] Sutton A P and Chen J 1990 *Phil. Mag. Lett.* **61** 139–46
[17] Andricioaei I and Straub J E 1996 *Phys. Rev.* E **53** R3055–8
[18] Doye J P K 2003 *J. Chem. Phys.* **119** 1136–47
[19] Qagin T, Kimura Y, Qi Y, Li H, Ikeda H, Johnson W L and Goddard W A 1999 *Mater. Res. Soc. Symp. Proc.* **554** 43–8
[20] Frenkel D and Smit B 1996 *Understanding Molecular Simulation* (San Diego, CA: Academic)
[21] Rieth M 2003 *Nano-Engineering in Science and Technology: an Introduction to the World of Nano-Design* (Singapore: World Scientific)

[22] Shumway J and Ceperley D M 2006 Quantum Monte Carlo methods in the study of nanostructures *Handbook of Theoretical and Computational Nanotechnology* vol 3, ed M Rieth and W Schommers (California, CA: American Scientific Publishers) pp 605–41
[23] Ceperley D M 2003 Metropolis methods for quantum Monte Carlo simulations *The Monte Carlo Method in the Physical Sciences*; *AIP Conf. Proc.* **690** 85–98
[24] Swaling R A 1972 *Thermoynamic of Solids* 2nd edn (New York: Wiley) pp 249–50
[25] Wu B, Heidelberg A, Boland J J, Sader J E, Sun X M and Li Y D 2006 *Nano Lett.* **6** 468–72
[26] Sun Y, Mayers B, Herricks T and Xia Y 2003 *Nano Lett.* **3** 955–60
[27] Sun W B and Xia Y 2007 *Acc. Chem. Res.* **40** 1067–76
[28] Blatchford C G, Campbell J R and Creighton J A 1982 *Surf. Sci.* **120** 435–55